ELSEVIER

Journal of Alloys and Compounds 330–332 (2002) 696–701

Journal of ALLOYS AND COMPOUNDS

www.elsevier.com/locate/jallcom

Engineering considerations in the use of catalyzed sodium alanates for hydrogen storage

G. Sandrock[a,c,*], K. Gross[a], G. Thomas[a], C. Jensen[b], D. Meeker[a], S. Takara[b]

[a]*Sandia National Laboratories, P.O. Box 969, MS 9402, Livermore, CA 94551, USA*
[b]*Chemistry Department, University of Hawaii, Honolulu, HI 96822, USA*
[c]*SunaTech, Inc., 113 Kraft Pl., Ringwood, NJ 07456, USA*

Abstract

The hydrogen storage properties of catalyzed $NaAlH_4$ (and associated Na_3AlH_6) were studied in relation to various practical engineering considerations. Properties measured were cyclic capacity, charging and discharging rates, thermal effects, gaseous impurities, volume changes, low temperature plateau pressures and detailed isothermal desorption kinetics over the temperature range 23–180°C. Two materials were evaluated, one mechanically milled with the liquid alkoxides $Ti(OBu^n)_4$ and $Zr(OPr^i)_4$ and one milled with dry $TiCl_3$ as catalyst precursors. The alkoxide-catalyzed materials had low reversible capacities and released significant levels of hydrocarbon impurities during H_2 discharge. These problems were virtually eliminated with the inorganic $TiCl_3$ catalyst precursor. The $NaAlH_4$ and Na_3AlH_6 decomposition kinetics of $TiCl_3$-catalyzed Na-alanate conform to Arrhenius behavior with activation energies of 79.5 and 97 kJ/mol H_2, respectively. Measured absorption and desorption kinetics were surprisingly good and it is shown that 3–4.5 wt.% H_2 can be stored and recovered in reasonable times at 100–125°C. It may even be ultimately possible to use the $NaAlH_4$ decomposition reaction to provide 3 wt.% H_2 at room temperature for low-rate applications. Published by Elsevier Science B.V.

Keywords: Hydrogen absorbing materials; Sodium alanates; $NaAlH_4$; Na_3AlH_6; Desorption kinetics; Engineering properties

1. Introduction

Catalyzed Na-alanates, and related ionic-covalent complex hydrides, offer hope to avoid the inherent gravimetric and thermodynamic limitations of traditional metallic or covalent hydrides as H_2 storage media [1–7]. An historic review of past R&D activity is given in these Proceedings [7]. The key to their exploitation is the following two-stage reaction:

$$NaAlH_4 \leftrightarrows 1/3Na_3AlH_6 + 2/3Al + H_2 \leftrightarrows NaH + Al + 3/2H_2 \qquad (1)$$

The first step consists of 3.7 wt.% H_2 release and the second step 1.9 wt.% for a theoretical net reaction of 5.6 wt.% reversible gravimetric H-storage. Such an achievement, especially if it could be accomplished below 100°C, would be of significant practical value for on-board H_2 storage for low-temperature fuel-cell vehicles.

The work presented here summarizes recent cooperative activities between Sandia National Labs and the University of Hawaii to understand the properties of mechanically catalyzed [3–6] (as opposed to chemically catalyzed [1,2]) Na-alanates with respect to practical H_2-storage applications in engineering devices. There are a number of engineering problems that must be understood and/or solved before the catalyzed alanates can be applied to practical H-storage. What are the practical H-capacities we can expect, relative to the 5.6-wt.% ideal of Eq. (1)? Are there *cyclic effects* on capacity? What are the *low-temperature kinetics*, given the fact the reaction steps in Eq. (1) must involve at least localized metal atom diffusion? Will they be high enough for application in vehicles and other devices? What are the *equilibrium plateau pressures at low temperature* (down to room temperature)? Because of low kinetics, we have had to rely on van't Hoff extrapolation from higher temperatures until now. Most importantly, a *macroscopic* 'engineering-scale' *catalyzed alanate bed* has never been made and tested. Are there any problems with large beds? What are the *reaction heat effects*? Can the alanate bed be melted or sintered during exothermic charging and what are the resultant changes in internal gas impedance effects? What are the *volume changes* associ-

---

*Corresponding author.
E-mail address: sandrock@warwick.net (G. Sandrock).

0925-8388/02/$ – see front matter Published by Elsevier Science B.V.
PII: S0925-8388(01)01505-5

ated with hydriding and dehydriding. Do the liquid organometallic or solid chloride catalyst precursors decompose in service, resulting in *contamination of the desorbed* H_2? Other fundamental aspects of our joint work on mechanically catalyzed alanates are presented elsewhere in this volume [7–9].

2. Experimental basics

The work reported here was done with $NaAlH_4$ to which was mixed 2 mol% each of liquid $Ti(OBu^n)_4$ (titanium(IV) butoxide, $Ti[O(CH_2)_3CH_3]_4$) and alcohol-dissolved $Zr(OPr^i)_4$ (zirconium(IV) propoxide, $Zr[OCH_2CH_2CH_3]_4$) or 2 mol% solid $TiCl_3$ by mechanical ball-milling. The use of the dual Ti–Zr catalyst system formula was based on the Hawaii observation that combined Ti- and Zr-doping resulted in maximum desorption kinetics for both steps of Eq. (1) [4]. Both the alkoxide and chloride additions decompose during ball-milling or service to likely form metallic (zero-valent) Ti/Zr, as is the case during solution doping [1,2]. In the solid $TiCl_3$ case, Cl is transferred from Ti to Na to form NaCl [7]. However, it was not clear from this study what form the Ti/Zr finally takes (e.g. elemental or alloyed with Al) and how it acts as an effective catalyst.

Hydrogen absorption/desorption studies were done using two experimental reactors. One represents what we call the '100 g scaleup reactor' designed to simulate the heat transfer and gas impedance conditions of a larger engineering bed. This 316 SS reactor has a 4.6-cm OD, 0.38-cm wall and 11.4-cm internal length. It was loaded with about 100 g of bicatalyzed $NaAlH_4$ as described above (78 g of $NaAlH_4$ and 22 g of $Ti(OBu^n)_4 + Zr(OPr^i)_4$). The $NaAlH_4$ was synthesized at Hawaii (2–20-μm particle size) and blended with the catalysts at Sandia using a few minutes of ball-milling. Ball-milling, even for longer times, did not result in much particle size reduction, but there was a tendency to form agglomerated clusters (150 μm) of the smaller particles [9]. The reactor had internal thermocouples but no internal heat exchange structure. The reactor was heated with an air furnace. Absorption kinetics and capacity were measured volumetrically and desorption measured with flow meters backed up by a wet test meter. The data below are presented in terms of wt.% H_2 normalized to the alanate weight only (i.e. not including the 22 wt.% Ti+Zr alkoxide catalysts).

Kinetics, capacities and plateau pressures were also obtained volumetrically with a carefully calibrated and instrumented Sieverts' apparatus using a smaller 316 SS reactor (1.3-cm OD×0.12-cm wall) containing about 1.5 g of catalyzed samples. The sample used was catalyzed with 2 mol% (5.5 wt.%) $TiCl_3$. This reactor also had a fine internal thermocouple located in the middle of the bed and was heated with external electrical heating tape.

Both the bicatalyzed 100-g bed and the 1.5 g $TiCl_3$-catalyzed beds were evaluated through five instrumented absorption/desorption cycles. (The wet chemical synthesis of the starting $NaAlH_4$ is artificially considered the first absorption half-cycle, 1A.) For the 100-g bed, absorption H_2 pressures generally ranged from 100 to 200 atm and nominal temperatures ranged from 125 to 165°C. Desorption was generally performed at 150–165°C against a 1 psig (1.07 atm) backpressure. For the 1.5-g bed, absorption was done at 82–90 atm H_2 pressure at 100–125°C. Desorption was done into evacuated volumes at backpressures well below the respective $NaAlH_4$ and Na_3AlH_6 plateaux. Exit H_2 was semiquantitatively analyzed for possible gaseous impurities. Selected samples were examined by surface analysis [9]. The reaction volume change was measured for the last desorption half-cycle of the 100-g bed, using the He displacement technique.

3. Results and discussion

3.1. Cyclic capacity and engineering rates

The measured absorption and desorption capacities of the 100-g scaleup bed are shown as a function of cycle number in Fig. 1. Generally good agreement was found between absorbed gas quantities and the amounts subsequently desorbed. However, cycle 1D (first discharge) showed a capacity of 6.0 wt.% H_2, in significant excess of

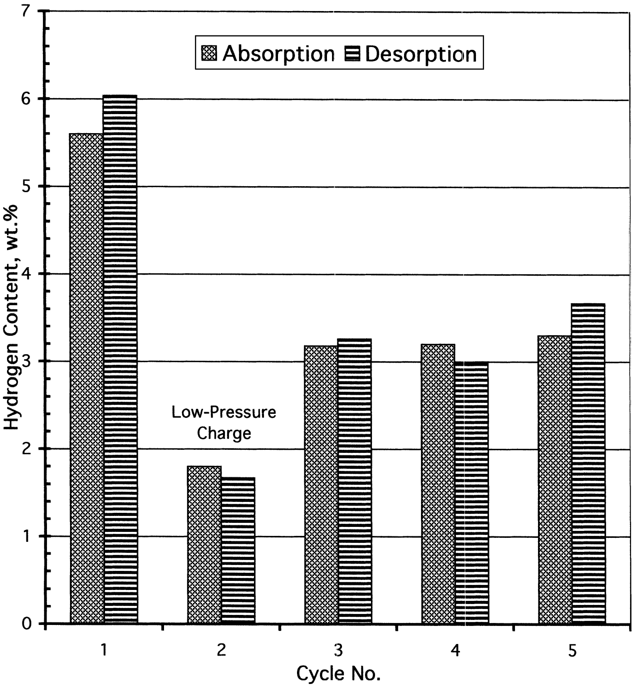

Fig. 1. Cyclic capacities of the 100 g $NaAlH_4$ scaleup bed mechanically doped with 2 mol% each of the liquid alkoxide catalyst precursors $Ti(OBu^n)_4$ and $Zr(OPr^i)_4$. Charging was done at 100–200 atm and 125–165°C, except for cycle 2 which was charged at only 14 atm (i.e. only through the Na_3AlH_6 phase).

the 5.6 wt.% theoretical value from Eq. (1). This is believed to be an indication of substantial quantities of non-H_2 impurities coming out of the bed during the first desorption (see Section 3.3 below). Cycle 2 was only a partial cycle because the charge pressure used was only 14 atm, well below the $NaAlH_4$ plateau pressure at 125°C and, hence, only the Na_3AlH_6 phase was formed. Cycles 3–5 show a serious capacity problem encountered not only with the 100 g scaleup bed but with other smaller samples we have tested with the liquid alkoxide catalysts. Cyclic capacity was only about 3 wt.%, well below the 5.6 wt.% expected for this system. X-ray diffraction measurements clearly showed that the low capacity is due to an inability to completely recharge to 100% $NaAlH_4$ (Eq. (1), full left reaction) [8]. There was no problem discharging to NaH+Al (Eq. (1), full right reaction). Although a range of applied pressures and starting temperatures were tried, in all cases charging was reasonably rapid, albeit incomplete. Most of the H_2 uptake was accomplished in the first hour or two, and the discharge was nearly as fast at 150–165°C, with desorption to NaH+Al occurring in about 3 h.

Because the low reversible capacity of direct alkoxide-catalyzed Na-alanate seemed to be related to organic impurities resulting from in situ alkoxide decomposition, we redirected activities toward the inorganic catalyst system $NaAlH_4$–2 mol% $TiCl_3$. Cyclic capacities for this system are shown in Fig. 2. Although full stoichiometric 5.6 reversible wt.% was not achieved, 4+ wt.% was consistently achieved, which is a considerable improvement over the liquid alkoxide results of Fig. 1. What appears to be a trend of lower capacities with cycle number is more likely an artifact related to variations in the time and temperature used for each half-cycle. For example, desorption 4D was not carried to completion (see Fig. 3), so naturally subsequent absorption 5A is also low. The final 180°C desorption (5D) was almost up to the capacity of the first 150°C desorption (1D), so the net 5-cycle loss of the $TiCl_3$-catalyzed composition seems to be small. We have not determined longer-term cycling effects for our mechanically doped samples, but they have been reported on solution doped samples [1,2].

3.2. Thermal effects

The high initial charging kinetics, combined with limited heat transfer, results in exothermic temperature excursions, well known for other 'fast' hydrides. For example, during half-cycle 4A of the 100-g bed, internal temperature rose within 1 min from 155 to 234°C. This is essentially the van't Hoff temperature for $NaAlH_4$ at the applied pressure of 172 atm H_2. It is important to recognize that the melting point of $NaAlH_4$ is only 182°C [10]; thus, any of that phase formed during initial charging would do so directly into the liquid form. This was confirmed because we could observe a brief and very clear 182°C thermal

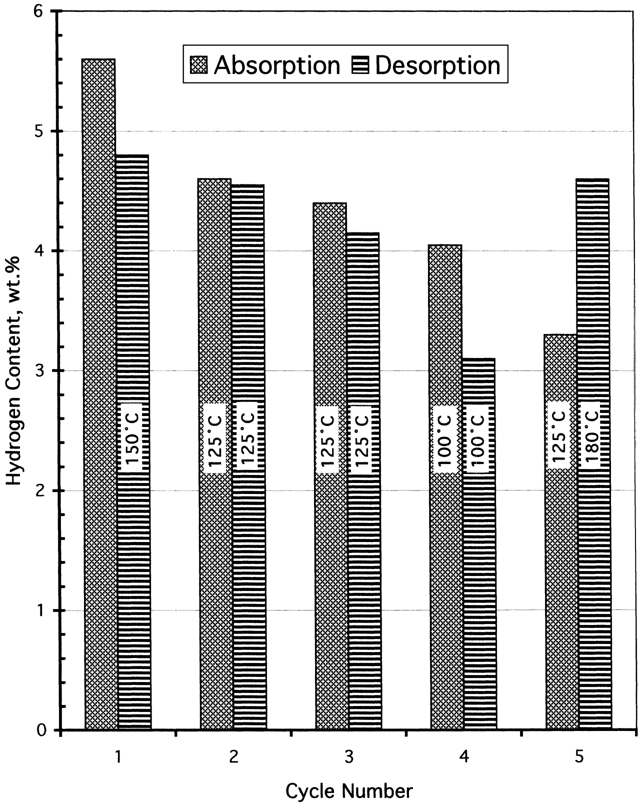

Fig. 2. Cyclic capacities of the 1.5-g bed of $NaAlH_4$ mechanically doped with 2 mol% $TiCl_3$ catalyst precursor. Charging was done at 82–90 atm at the temperatures indicated.

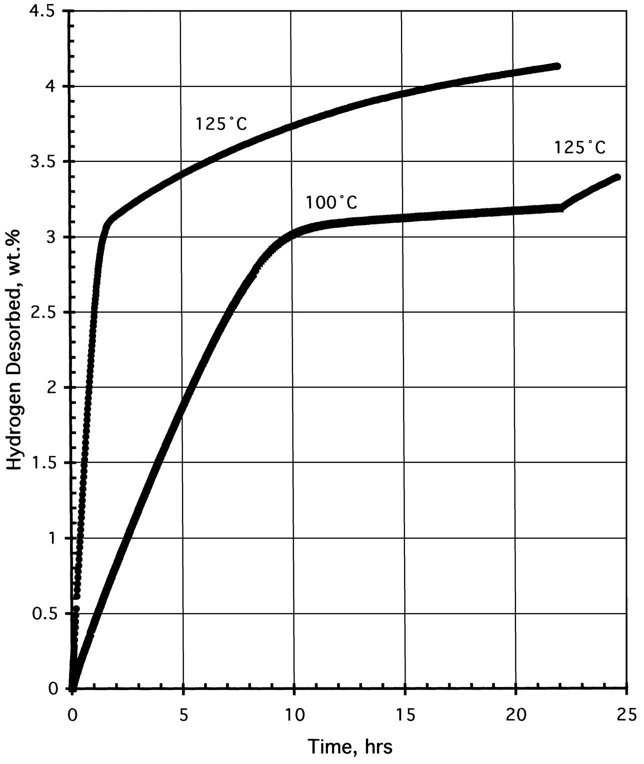

Fig. 3. Desorption curves at 125 and 100°C for the 1.5-g bed of $NaAlH_4$ mechanically doped with 2 mol% $TiCl_3$ catalyst precursor.

arrest during cooling from the initial high temperature excursion [7].

It is natural to ask if such melting could be detrimental to the subsequent performance of the alanate bed. The answer seems to be ‘no’ or at least ‘not much’. We have not seen any negative effects of partially melting the 100-g bed at least three times. In fact, there may be a benefit of partial melting. We opened the reactor between cycles 4 and 5 and found the bed to be sintered into a porous, reasonably strong mass (density$\approx$0.85 g/cm^3). Such a structure may have distinct advantages relative to limiting particulate migration, packing and expansion, as well as maintaining stable internal gas impedance.

3.3. Gaseous impurities

The direct addition of the catalysts in the form of liquid organometallic alkoxides [3,4] seems to result in serious problems relative to the purity of the desorbed H_2 and may be a contributing cause to the low cyclic capacity we see (Fig. 1). The first desorption (1D) of the 100-g scaleup bed resulted in a measured quantity of exit gas in excess of the stoichiometric 5.6 wt.% H_2. Hence, during subsequent desorption half-cycles, semiquantitative analyses of the desorbed gas composition were done by RGA (residual gas analysis (mass spectroscopy)) and occasionally by GC (gas chromatography). Several impurity peaks were evident during all of the desorptions. An RGA/GC analysis taken of cycle 2D desorbed gas showed that at least the hydrocarbons butane (C_4H_{10}) and propane (C_3H_8) were present in the hydrogen. Thus the $Ti(OBu^n)_4$ and $Zr(OPr^i)_4$ dopants seem to be decomposing during cycling. EDS (X-ray energy dispersive spectroscopy) analysis of the material clearly showed that most of the O-atoms introduced with the $Ti(OBu^n)_4+Zr(OPr^i)_4$ catalysts remain on the hydride surface after both stages of desorption [9], presumably forming oxides of Na, Al and/or Ti/Zr. It may be that surface damage associated with this oxygen is a contributing factor to the much lower than stoichiometric cyclic capacity we see with liquid alkoxide doped Na-alanate.

We believe the high impurity level of the output H_2 (not to mention possible surface damage from the catalysts) constitutes a fatal flaw to the otherwise convenient process of wet-mechanical-alkoxide-doping of Na-alanate. One likely application for an onboard storage bed will be the PEM fuel-cell which is not very tolerant of impurities in the H_2 fuel, especially carbonaceous species that might include or lead to CO. It may be possible to remove the impurities by vacuum bakeout and repeated cycling, but we feel this will never be completely effective or economical. This is because we observed significant impurity levels even after five cycles and temperature excursions above 200°C. Furthermore, this does not address the problem of capacity loss that may be due to damage by the by the organic-based catalysts. For this reason we have redirected our work toward inorganic catalyst species. It is encouraging that our preliminary analysis results on the dry-$TiCl_3$-doped sample showed insignificant impurity levels, even during the first desorption half-cycle.

3.4. Hydriding volume changes

For the traditional metallic hydrides, hydride/dehydride volume changes are large, typically on the order of 25%. Because such large volume changes pose engineering problems (e.g. bed packing, expansion, deformation, etc.), it is important to know how the complex alanates behave. From published X-ray densities, the first stage of decomposition ($NaAlH_4 \rightarrow 1/3Na_3AlH_6 + 2/3Al$) would be expected to give a 30.3% contraction and the second stage ($1/3Na_3AlH_6 + 2/3Al \rightarrow NaH + Al$) an expansion of 13.8%. The net ΔV for the complete dehydriding reaction of Eq. (1), including consideration of the Al produced in both stages, would then be expected to be -16.5%. The actual volume change measured during the 100-g bed dehydriding half-cycle 5D was -14.7%, slightly lower than predicted. The small difference is presumably due to the somewhat low capacity (3.6 wt.%) of the bed. The relatively small volume change and hydrided starting material makes designing the container easier and also allows a higher packing compared to traditional hydrides.

3.5. Desorption kinetics and Arrhenius analyses

The desorption kinetics of $NaAlH_4$ and Na_3AlH_6 (as per Eq. (1)) are less than desired for many applications, e.g. to supply fuel for a fuel-cell vehicle where the waste heat for the required desorption enthalpy ΔH is available at less than 100°C. There remain further needs to increase kinetics through new catalysts, particle size reductions and other possibilities. As a baseline, we have carefully determined the kinetics of both the $NaAlH_4$ and Na_3AlH_6 decomposition reactions over wide ranges of temperature (23–150°C for $NaAlH_4$ and 60–180°C for Na_3AlH_6) using the small $NaAlH_4$–2 mol% $TiCl_3$ sample. It should be mentioned that kinetics are strongly influenced by particle size [2]. The sample we used was high-energy ball-milled for 3 h to give relatively fine powder as well as intimate mixing of the solid catalyst particles. After the desorption kinetic testing (half-cycle 5D in Fig. 2) the sample was a porous structure with pore spacing on the order of 0.5 μm. With careful calibration of our Sieverts’ apparatus, and careful treatment of the data, we were able to precisely measure H_2 desorption rates down to 10^{-4} wt.%/h.

Examples of desorption curves are shown in Fig. 3 for 125 and 100°C. They are typical of measurements taken at all temperatures and show two distinct features: (1) two stages of desorption, both of which are approximately linear with time over much of each desorption range, and (2) a pronounced decrease in desorption rate at about 3.0–3.1 wt.% H_2. The two stages represent $NaAlH_4$ and

Na_3AlH_6 decompositions, respectively, with the latter markedly slower at each temperature. In addition, temperature can be seen to have a marked effect on the kinetics of both reactions. The 100°C Na_3AlH_6 decomposition was not taken to completion; instead just before terminating the test, we abruptly increased the temperature from 100 to 125°C. It can be seen that H_2 desorption increased to the same rate as the desorption curve measured isothermally at 125°C at the equivalent wt.% level.

Thermally activated reactions would be expected to show temperature dependence consistent with the Arrhenius equation

$$\text{Rate} = k_0 \exp(-Q/RT), \tag{2}$$

where we express rate in convenient engineering terms of wt.%/h, k_0 is the rate constant, Q is the thermal activation energy, R is the gas constant (8.32 J/mol K) and T is absolute temperature (K). The measured rates of both the $NaAlH_4$ decomposition (23–150°C) and Na_3AlH_6 (60–180°C) are plotted in Arrhenius form (log rate versus $1/T$) in Fig. 4. As can be seen, excellent exponential fits apply to both decomposition steps over the entire temperature ranges experimentally studied. Thus the Arrhenius equations for the decomposition reaction can be written as follows:

$$\text{Rate}\,(NaAlH_4) = 7.19 \times 10^{10} \exp(-9559/T) \tag{3}$$

$$\text{Rate}\,(Na_3AlH_6) = 5.33 \times 10^{11} \exp(-11\,652/T) \tag{4}$$

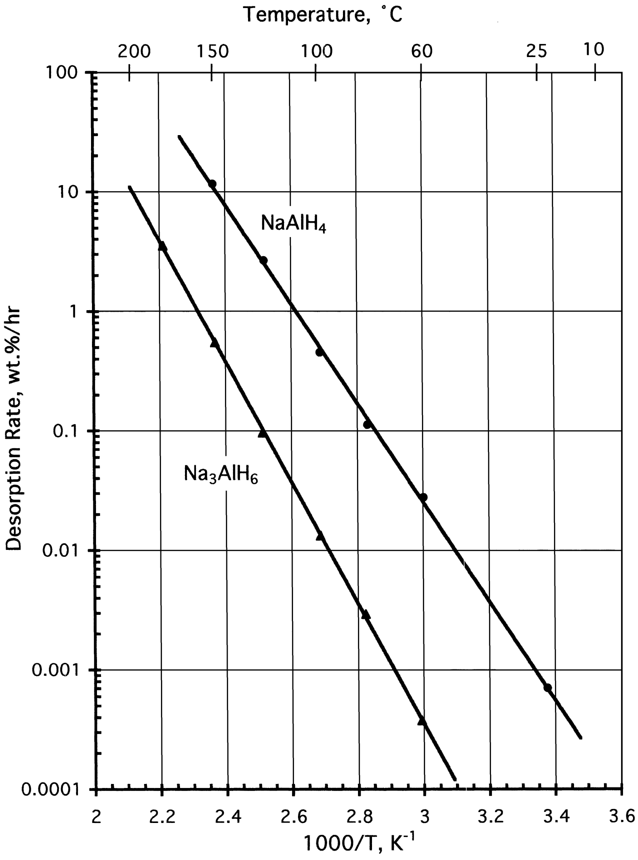

Fig. 4. Arrhenius plots of the desorption kinetics of $NaAlH_4$ and Na_3AlH_6 (steps 1 and 2 of Eq. (1)): 1.5-g sample mechanically doped with 2 mol% $TiCl_3$ catalyst precursor.

The corresponding activation energies Q are 79.5 and 96.9 kJ/mol H_2 for the $NaAlH_4$ and Na_3AlH_6 decomposition steps, respectively. In terms of Al stoichiometry changes, the corresponding values of Q are 119.3 and 145.3 kJ/mol Al. These values are close to the reported Al self-diffusion activation energy of 142.4 kJ/mol Al [11], but of course this does not prove that diffusion-controlled Al precipitation and/or growth are the sole rate controlling mechanisms for $NaAlH_4$ and Na_3AlH_6 decompositions. The thermally independent rate constant k_0 varies by almost an order of magnitude between the two steps. Particle size effects and catalytic influences probably affect k_0 more than Q. Arrhenius analyses should provide a valuable method for characterizing catalysis or processing variables.

To our knowledge, this is the first time that $NaAlH_4$ has been reported to decompose at room temperature, and that quantitative low temperature H_2 desorption kinetics have been measured. This has practical significance, for example the possibility of a high-capacity catalyzed-$NaAlH_4$ H_2 supply for long-duration, low-demand devices that use H_2. Examples might be low-power remote fuel-cells or portable gas analyzers. Although we have not yet fully demonstrated it, it seems possible that we could achieve 3 available wt.% H_2 at room temperature from $NaAlH_4 \rightarrow Na_3AlH_6$ desorption. It would take significant time, of course. For example, the $TiCl_3$-catalyzed sample used for Fig. 4 would require at least 3750 h (156 days) to release 3 wt.% H_2. But hopefully future improvements in kinetics will accrue with more R&D.

3.6. Low temperature van't Hoff data

The reasonably high kinetics at low temperatures allowed the reliable determination of equilibrium desorption plateau pressures down to room temperature for the $NaAlH_4$ phase. These data are presented elsewhere [7]. The measured values confirm the extrapolation of earlier high-temperature data. We have now accurately demonstrated that the temperature for 1 atmosphere (absolute) hydrogen desorption pressure is 33°C. This is a very convenient temperature for ambient temperature application. However, for many applications such as fuel-cell electric vehicles we must now increase kinetics by two or three orders of magnitude.

4. Summary and conclusions

1. The Ti + Zr alkoxide mechanical catalyst doping procedure has the following engineering problems for H_2-storage applications:
   (A) The required catalysts are too heavy. Standard loadings of 2 mol% each results in a 22 wt.% burden on the bed.
   (B) The liquid organometallic catalyst precursors contribute to significant hydrocarbon contamination of the exit H_2, in particular butane and propane.
   (C) The oxygen from the alkoxide catalysts at least partially remains in the bed, perhaps damaging surfaces and causing less than ideal cyclic capacity.
2. The dry-doping $TiCl_3$ catalyst procedure largely eliminates the high catalyst weight, low capacity and contamination problems noted in above with the alkoxide catalysts.
3. The initial absorption kinetics were so high that reaction self-heating was significant, easily exceeding the 182°C melting temperature of $NaAlH_4$. Partial melting of the alanate bed did not appear to hinder subsequent absorption/desorption (A/D) kinetics. On the contrary, it results in a moderately sintered porous structure that effectively fixes the particulates, thus simplifying large bed design.
4. The A/D volume changes of alanate beds are lower than conventional metallic hydrides. This also simplifies large bed design and may allow higher hydride fillings.
5. $NaAlH_4$ has measurable desorption kinetics down to room temperature; it may even be possible to store and generate 3 wt.% H_2 for ambient temperature applications where rate demands are very low.
6. The desorption of H_2 from $NaAlH_4$ and Na_3AlH_6 is essentially linear with time and follows Arrhenius thermal activation kinetics. Activation energies were found to be 79.5 and 97 kJ/mol H_2 for $NaAlH_4$ and Na_3AlH_6 decompositions, respectively.

Acknowledgements

We thank Tim Sage for help in constructing and operating the high-pressure apparatus used for the 100-g scaleup bed. We gratefully acknowledge financial support of the US DOE Hydrogen Program. More aspects of this work can be found in our latest Annual Reports to the DOE [12,13].

References

[1] B. Bogdanovic', M.J. Schwickardi, J. Alloys Comp. 253 (1997) 1.
[2] B. Bogdanovic', R.A. Brand, A. Marjanovic', M. Schwikardi, J. Tölle, J. Alloys Comp. 302 (2000) 36.
[3] C.M. Jensen, R.A. Zidan, N. Mariels, A.G. Hee, C. Hagen, Int. J. Hydrogen Energy 24 (1999) 461.
[4] R.A. Zidan, A.G. Hee, C.M. Jensen, J. Alloys Comp. 285 (1999) 119.
[5] C.M. Jensen, K.J. Gross, Appl. Phys. A 72 (2001) 213.
[6] A. Zaluska, L. Zaluski, J.O. Ström-Olsen, J. Alloys Comp. 298 (2000) 125.
[7] K.J. Gross, G.J. Thomas, C.M. Jensen, J. Alloys Comp. 330–332 (2002) 683.
[8] K.J. Gross, G. Sandrock, G. Thomas, J. Alloys Comp. 330–332 (2002) 691.
[9] G.J. Thomas, K.J. Gross, N.Y.C. Yang, C. Jensen, J. Alloys Comp. 330–332 (2002) 702.
[10] T.N. Dymova, Y.M. Dergachev, V.A. Sokolov, N.A. Grechanaya, Dokl. Akad. Nauk SSSR 224 (1974) 591.
[11] T.S. Lundy, J.S. Murdock, J. Appl. Phys. 33 (1962) 1671.
[12] K.J. Gross, G. J. Thomas, G. Sandrock, Hydride Development for Hydrogen Storage, Proceedings of the 2000 Hydrogen Program Review, NREL Conf. Rept. NREL/CP-570-28890, http://www.eren.doe.gov/hydrogen/docs/28890toc.html
[13] C. Jensen, S. Takara, Catalytically Enhanced Systems for Hydrogen Storage, Proceedings of the 2000 Hydrogen Program Review, NREL Conf. Rept. NREL/CP-570-28890, http://www.eren.doe.gov/hydrogen/docs/28890toc.html